frontiers in Marine Science

ORIGINAL RESEARCH
published: 30 November 2021
doi: 10.3389/fmars.2021.740416

Photobleaching and Recovery of Symbiodiniaceae *Effrenium voratum* SCS01 Reveals Life Form Transformation Under Thermal Stress

*Sanqiang Gong[1,2], Gang Li[1,2], Xuejie Jin[1], Dajun Qiu[1,2], Jiayuan Liang[3], Kefu Yu[3], Yehui Tan[1,2], Xiao Ma[1,2] and Xiaomin Xia[1,2]**

[1] Key Laboratory of Tropical Marine Bioresources and Ecology and Guangdong Provincial Key Laboratory of Applied Marine Biology, South China Sea Institute of Oceanology, Chinese Academy of Sciences, Guangzhou, China, [2] Southern Marine Science and Engineering Guangdong Laboratory (Guangzhou), Guangzhou, China, [3] Coral Reef Research Center of China, Guangxi University, Nanning, China

OPEN ACCESS

Edited by:
Satya Panigrahi,
Indira Gandhi Centre for Atomic Research (IGCAR), India

Reviewed by:
Uma VS,
Indira Gandhi Centre for Atomic Research (IGCAR), India
Anthony William Larkum,
University of Technology Sydney, Australia

***Correspondence:**
Xiaomin Xia
xiaxiaomin@scsio.ac.cn

Specialty section:
This article was submitted to Marine Biology, a section of the journal Frontiers in Marine Science

Received: 13 July 2021
Accepted: 10 November 2021
Published: 30 November 2021

Citation:
Gong S, Li G, Jin X, Qiu D, Liang J, Yu K, Tan Y, Ma X and Xia X (2021) Photobleaching and Recovery of Symbiodiniaceae Effrenium voratum SCS01 Reveals Life Form Transformation Under Thermal Stress. Front. Mar. Sci. 8:740416. doi: 10.3389/fmars.2021.740416

Dinoflagellates in the family Symbiodiniaceae contain a number of species and play an important role in the establishment of coral reef ecosystems in oligotrophic marine waters. *Effrenium voratum* is likely an exclusively free-living and heterotrophic species of Symbiodiniaceae. How this species responds and acclimates to warming is largely unknown. The present study experimentally established the phenotypic landscapes related to the photobleaching and recovery processes of *Effrenium voratum* SCS01 following thermal stress. We found that thermal stress bleached the plastids of *E. voratum* SCS01 and caused the cells to become lighter in color. Thereafter, the bleached cells recovered rapidly when they returned to the optimal temperature. The dominant life form of *E. voratum* SCS01 shifted from mastigote cells to coccoid cells then returned to mastigote cells. Transcriptome analysis revealed that the photobleaching of *E. voratum* SCS01 was due to increased degradation and decreased biosynthesis of photosynthetic pigments. The thermally induced life form changes were related to the downregulation of genes for cell motility. Our results revealed the mechanism of photobleaching in *E. voratum* SCS01 and indicated life form transformation as a newly identified survival strategy of *Effrenium voratum* SCS01 under thermal stress.

Keywords: Symbiodiniaceae, *Effrenium voratum*, photobleaching, life form, warming

INTRODUCTION

Photosynthetic dinoflagellates in the family Symbiodiniaceae contain multiple species and play important roles in the establishment of coral reef ecosystems in oligotrophic marine waters (Sully et al., 2019). Symbiodiniaceae members were initially considered a single pandemic species of zooxanthellae (*Symbiodinium microadriaticum*) based on morphological analyses (Freudenthal, 1962). Subsequent understanding of the diversity of Symbiodiniaceae changed significantly due to sequence-based molecular analyses, and Symbiodiniaceae were divided into nine phylogenetically supported clades (A–I) (Pochon et al., 2014). Recently, Symbiodiniaceae clades

were formally described as different genera based on their genetic and ecological characteristics (i.e., *Symbiodinium*, *Breviolum*, *Cladocopium*, *Durusdinium*, *Effrenium*, *Fugacium,* and *Gerakladium*) (LaJeunesse et al., 2018). Among these Symbiodiniaceae members, *Symbiodinium*, *Breviolum*, *Cladocopium, Durusdinium,* and *Gerakladium* are primarily endosymbioses with reef building corals, and each of these genera include multiple species and a number of informally described molecular types (LaJeunesse et al., 2018). The genus *Effrenium* currently contains just one species, the exclusively free-living (non-symbiotic) *E. voratum* (LaJeunesse et al., 2018; Gong et al., 2021). This species uses its tubule peduncle to graze on bacteria and other unicellular eukaryotes, creates blooms under certain circumstances, uniquely maintains a cell life cycle with more mastigote cells (flagellated cells) than coccoid cells (vegetative cells) compared to other Symbiodiniaceae and is distributed in the Pacific and Atlantic Oceans (Chang, 1983; Jeong et al., 2012, 2014; Yamashita and Koike, 2013; LaJeunesse et al., 2018; Gong et al., 2021).

A significant number of studies using cultures of the Symbiodiniaceae have provided a tremendous amount of insight into the environmental responses of the endosymbionts of corals and other reef organisms (Rehman et al., 2016; Szabó et al., 2017; Buerger et al., 2020). Various cellular processes have been proposed as the target of coral bleaching in the endosymbiotic Symbiodiniaceae (i.e., *Symbiodinium*, *Breviolum*, *Cladocopium,* and *Durusdinium*) under elevated temperature, including production of reactive oxygen species (ROS) (Lesser, 2019), photosystem (PS) II reaction centers (Jeans et al., 2014), PSII repair (Takahashi et al., 2013) and the Calvin cycle (Hill et al., 2014). For the exclusively free-living species of Symbiodiniaceae *E. voratum*, related studies are limited. One previous study examined the physiological responses of *E. voratum* to two types of phosphates (Tian-Tian et al., 2019). Li et al. (2021) recently explored the physiological and molecular responses of *E. voratum* to N deficiency or a nitrate (NO_3^-) to ammonium (NH_4^+) switch. However, the response and acclimation of *E. voratum* to elevated temperatures due to ocean warming are largely unknown. Studying the responses, acclimation and/or adaptation of different Symbiodiniaceae taxa to ocean warming is important to help predict which Symbiodiniaceae species will be more resistant to ocean warming and reveal the cause of diversity of Symbiodiniaceae taxa from an environmental acclimation perspective. It is also possible to exploit their thermal stress acclimation or adaptation strategies to construct thermally tolerant Symbiodiniaceae species (Buerger et al., 2020).

The present study explored the phenotypic landscapes related to the photobleaching and recovery of *E. voratum* to reveal the cellular and molecular mechanisms related to the acclimation of free-living *E. voratum* to thermal stress. We isolated *Effrenium voratum* SCS01 from tropical coral reefs of the South China Sea and exposed it to different temperature gradients to assess its physiological responses to temperature variations. A short-term photobleaching and recovery experiment was also performed in which *E. voratum* SCS01 was initially cultured at its optimal growth temperature of 26°C, followed by exposure to thermal stress at 32°C for several days. *E. voratum* SCS01 was returned to the optimal growth temperature. Dynamic variations in cellular morphology coupled with pigment degradation and synthesis were also recorded in *E. voratum* SCS01 at different temperatures. Our data provide new insights into the life forms of *E. voratum* SCS01 and their roles in its acclimation to thermal stress.

MATERIALS AND METHODS

Isolation of Symbiodiniaceae Strains and Culture Protocol

The algal culture used in this study was isolated from tropical coral reefs of the South China Sea (E109.476, N18.211°) according to our previous methods (Gong et al., 2018, 2019). The unialgal strain of symbiotic Symbiodiniaceae was obtained according to Xiang's method (Xiang et al., 2013). The 18 S rRNA sequence of the culture was amplified using the primer pair ss5 and ss3z (Rowan and Powers, 1991) and was used as the query for a BLAST search against the National Center for Biotechnology Information (NCBI) database [1] with the default settings. The results showed that the 18 S rRNA gene sequence (**Supplementary File 1**) of the culture was highly similar to *E. voratum* SMFL (HE653238.1), with 98.6% identity and 100% query coverage. Therefore, the culture was named *E. voratum* SCS01 (**Supplementary Figure 1**).

Stock cultures of *E. voratum* SCS01 were maintained in 250-mL flasks with 100 mL of f/2 medium (Guillard and Ryther, 1962) at an *in situ* temperature of 26°C under a light intensity of 90 μmol photon m^{-2} s^{-1} and a light:dark cycle of 12 h:12 h.

The growth of *E. voratum* SCS01 at different temperatures was determined by inoculating the exponential-phase cells in 500-mL flasks with 250 mL of f/2 medium, followed by incubation at 20, 23, 26, 29, or 32°C for 10 days under the same light intensity and light:dark cycle indicated above.

To monitor the photobleaching and recovery of *E. voratum* SCS01, its cells were initially cultured at the optimal growth temperature (26°C) for 4 days. Exponential-phase cells were gently centrifuged (5,000 rpm, 5 min) and transferred to 3 500-mL flasks with 250 mL of f/2 medium. The flasks were cultured at 32°C. After 6 days of incubation, the cells cultured at 32°C were harvested and transferred to fresh medium as described above and cultured again at 26°C.

Growth and Morphology

At 18:00 every day, 1-mL aliquots of the cultures in each flask under different temperature treatments were collected and fixed with glutaraldehyde at a final concentration of 2.5%, and cell numbers were counted under a microscope (Leica DMRXA, Germany). The exponential growth phase was determined, and the maximal specific growth rate was calculated following Mou's method (Mou et al., 2017). The morphology of *E. voratum* SCS01 cells was recorded using a fluorescence microscope (Leica DMRXA, Germany) under bright-field conditions and/or fluorescent light. The subcellular structures of *E. voratum* SCS01 cells were imaged via transmission electron

[1] https://blast.ncbi.nlm.nih.gov

microscopy according to our previously reported method (Gong et al., 2018).

Chlorophyll Fluorescence, Photosynthetic, and Respiration Rates

The maximum photochemical efficiency of photosystem II (PS II) of *E. voratum* SCS01 was measured using a pulse-amplitude modulated (PAM) fluorometer (Water-PAM WALZ, Germany) after dark adaptation for 20 min in a custom-made acrylic black box at room temperature. Briefly, we measured the maximal chlorophyll fluorescence (F_m) of the dark-adapted cells under a saturating blue light pulse (3,000 μmol photons m^{-2} s^{-1}, 1 s), and we measured their minimal fluorescence (F_O) in the presence of weak, modulated measurement light. We then calculated the maximum PSII photochemical quantum yield (*Fv/Fm*) (van Kooten and Snel, 1990) as follows:

$$\frac{F_v}{F_m} \quad \frac{F_m - F_O}{F_m}$$

The photosynthetic and respiration rates of *E. voratum* SCS01 cells were measured using the oxygen electrode method. Culture was collected from each flask, centrifuged (5,000 × g, 5 min) (5804 R Eppendorf, Germany), resuspended to 5 mL in remaining media, and dark adapted for 5 min in a chamber with temperature control to the same as growth temperature. The incident irradiance in the chamber was supplied by LED flexible rope lights and measured using a microspherical quantum sensor (QSL2100, Biospherical Instruments Inc., United States). The decline in oxygen concentration under dark conditions and the increase in oxygen concentration under illumination (90 μmol photon m^{-2} s^{-1}) were tracked using a liquid oxygen electrode (Chlorolab 2, Hansatech Instrument Ltd., United Kingdom). The photosynthetic and respiration rates of *E. voratum* SCS01 were calculated according to the oxygen increase and decline rates (μmol O_2 S^{-1} per 10^6 cells), respectively.

Pigments, Carbohydrates, and Lipids

E. voratum SCS01 cells in 100-mL aliquots of the cultures under different temperature treatments were collected via centrifugation (5,000 rpm, 5 min) and dried in a vacuum freeze dryer (SCIENTZ-18N, China). Freeze-dried cells were used to assess the biochemical composition (i.e., pigment, total carbohydrates and total lipids) under each treatment. To measure pigment contents, freeze-dried cells were extracted in 7 mL of 100% acetone for 24 h, and chlorophyll a and carotenoid contents were determined following Dere's method (Dere et al., 1998). Total carbohydrates were extracted from freeze-dried *E. voratum* SCS01 cells using 1 N H_2SO_4 at 80°C. The total carbohydrate content was determined via the phenol-sulfuric acid method proposed by DuBois et al. (1956) using glucose as a standard. The extraction of total lipids and the determination of their contents were performed using a modified version of the Khozin-Goldberg's method (Khozingoldberg et al., 2005). Pigment, total carbohydrate and total lipid contents were calculated as nanograms per cell.

RNA Sequencing and Gene Transcription

E. voratum SCS01 cells for the photobleaching and recovery experiments were collected via centrifugation (5,000 rpm, 5 min) on day 4 of incubation at 26°C, on day 2 and day 6 after transfer to 32°C, and on day 4 after being returned to 26°C. The cell pellets were immediately frozen in liquid nitrogen then stored at −80°C for further RNA extraction. Total RNA was extracted from *E. voratum* SC01 cells using the TRIzol method (Invitrogen, Australia) (Rosic and Hoegh-Guldberg, 2010). RNA quantity and integrity were analyzed using a NanoDrop ND-1000 spectrometer (Wilmington, DE, United States) and an Agilent 2100 Bioanalyzer (Santa Clara, CA, United States). RNA samples with high purity (OD260/280 between 1.8 and 2.2) and high integrity (RNA integrity number (RIN) > 7.5) were used for further cDNA library construction. cDNA library construction and the sequencing and quality control of raw sequences were performed according to our previous study (Gong et al., 2020). The raw sequence data sets (a total of 12 sequencing libraries, the statistical information of RNA-seq data sets were supplied in **Supplementary Table 1**) produced in this study were deposited in the Sequence Read Archive (PRJNA699996) of the NCBI (see text footnote 1).

The obtained clean reads were assembled *de novo* with Trinity v2.1.1 software using the default parameters (Haas et al., 2013), and the statistical information of *de novo* assembled unigenes is supplied in **Supplementary Table 2** and **Supplementary File 2**. The expression levels of the unigenes (in fragments per kilobase of exon model per million mapped fragments, FPKM) were calculated using RSEM provided within the Trinity package (Li and Dewey, 2011). All unigenes were annotated using the Basic Local Alignment Search Tool (BLAST) algorithm with a cutoff *E*-value of 10^{-5} based on the NCBI non-redundant protein (Nr) database. The sequences of the identified differentially expressed genes (DEGs) were also subjected to BLAST searches against entries in the Swiss-Prot, Kyoto Encyclopedia of Genes and Genomes (KEGG), Eukaryotic Orthologous Groups of proteins (KOG) and Gene Ontology (GO) databases (**Supplementary File 2**). The annotation files are supplied in **Supplementary File 3**. The analysis of DEGs in the samples was performed using the DEGseq2 method, with a threshold *q*-value of < 0.001. Genes with a log2 fold change (LogFC) ≥ 1, false discovery rate (FDR) < 0.05 and FPKM ≥ 3 (in at least one group) were considered significant DEGs.

Statistical Analysis

All of the data are recorded as the means ± standard deviation values from at least 3 independent biological replicates. One-way analysis of variance (ANOVA) with Tukey's test was used to analyze the experimental data, and the differences were considered significant at $P < 0.05$. All analyses and visualizations of the results were performed using the vegan and pheatmap packages in R software (R 3.1.2) and/or Origin 8.5 software.

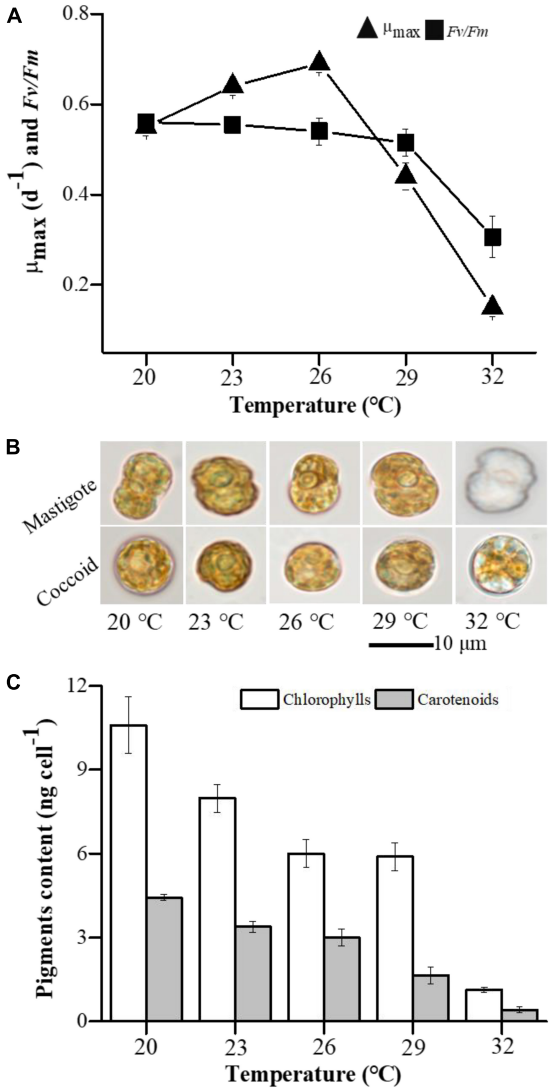

FIGURE 1 | Effect of temperature variations on the growth, photosynthesis and cell morphology of *E. voratum* SCS01. **(A)** Variations in the maximal growth rate (μmax) and the photochemical efficiency of PSII (*Fv/Fm*) in *E. voratum* SCS01. **(B)** Representative micrographs (bright field) of mastigote and coccoid cells of *E. voratum* SCS01 (day 6). **(C)** Variations in pigment content in *E. voratum* SCS01 (day 6).

RESULTS

Growth, Photosynthesis and Cell Morphology at Different Temperatures

The maximal specific growth rate (μ_{max}) of *E. voratum* SCS01 increased from 0.55 to 0.69 d^{-1} when the temperature increased from 20 to 26°C and then decreased to 0.15 d^{-1} with a further increase in temperature to 32°C (**Figure 1A** and **Supplementary Figure 2**). The *Fv/Fm* ratio of *E. voratum* SCS01 gradually decreased from 0.64 to 0.61 as the temperature increased from 20 to 29°C and then dramatically declined to 0.47 at 32°C (**Figure 1A**). Visible plastid photobleaching was observed in *E. voratum* SCS01 coccoid and mastigote cells at 32°C (**Figure 1B** and **Supplementary Figure 3**), which was supported by a significant decline in pigment content (chlorophyll and carotenoid contents) (**Figure 1C**) and *Fv/Fm* values (**Figure 1A**).

Physiological and Morphological Changes During Bleaching and Recovery

The physiological and morphological changes observed in *E. voratum* SCS01 during the bleaching and recovery processes are shown in **Figure 2**. Cell counts increased from 2.3×10^5 cells mL^{-1} to 2.5×10^6 cells mL^{-1} from days 0 to 4, when *E. voratum* SCS01 was incubated at 26°. After transfer to 32 °C, cell counts decreased dramatically to 4.6×10^5 cells mL^{-1} on day 10. After 4 days of recovery at 26°C, the cell count increased again to 1.5×10^6 cells mL^{-1} (**Figure 2A**). The *Fv/Fm* value exhibited a similar variation trend. Morphological measurements clearly showed pigment loss in mastigote and coccoid cells on day 6 and day 10 due to thermal stress (32°C), but the cells recovered a brownish color after being returned to 26°C for 4 days (day 14) (**Figure 2B** and **Supplementary Figure 4**). In accordance with the observed morphological changes, cellular chlorophyll and carotenoid contents decreased with thermal stress then increased after the stress was removed (**Figure 2C**). The net photosynthetic rate was lower, and the respiration rate was higher at 32°C than at 26°C in the initial and recovery cultures (**Figure 2D**).

Two distinct life forms of *E. voratum* SCS01 were identified during the bleaching and recovery periods, including coccoid cells (vegetative) and mastigote cells (flagellated) (**Figure 3A** and **Supplementary Figure 5**). Mastigote cells dominated the initial cultures (day 4) and constituted over 85% of the total cells. At this stage, coccoid cells accounted for approximately 10% of the total cells (**Figure 3B**). During the bleaching period (days 4 and 10), the proportion of coccoid cells increased to over 50%. The proportion of mastigote cells simultaneously declined to 13% (**Figure 3B**). When the photobleached *E. voratum* SCS01 cells were returned to 26°C, the proportions of coccoid and mastigote cells recovered to the levels observed in the initial period (day 4).

Transcriptomic Responses to Temperature Changes

The transcriptomes of *E. voratum* SCS01 were analyzed in different stages of bleaching and recovery processes (**Figure 3C** and **Supplementary File 4**). Three genes related to cell motility mediated by the flagellum were downregulated during the bleaching period (**Figure 3C**). These genes encoded sperm motility kinase 2B (2.1-fold downregulation in day 10 bleaching samples compared to the initial day 4 samples, q-value < 0.001), sperm acrosomal protein FSA-ACR.1 (2.5-fold downregulation in day 10 bleaching samples compared to the initial day 4 samples, q-value < 0.001), and cation channel sperm-associated protein 1 (2.0-fold downregulation in day 10 bleaching samples compared to the initial day 4 samples, q-value < 0.001). These results were consistent with the decrease in mastigote cells during the bleaching period. Genes encoding MEI2 protein family members (ML1, ML2, ML3, ML4, and ML5, over 2.1-fold downregulation in day 10 bleaching samples compared

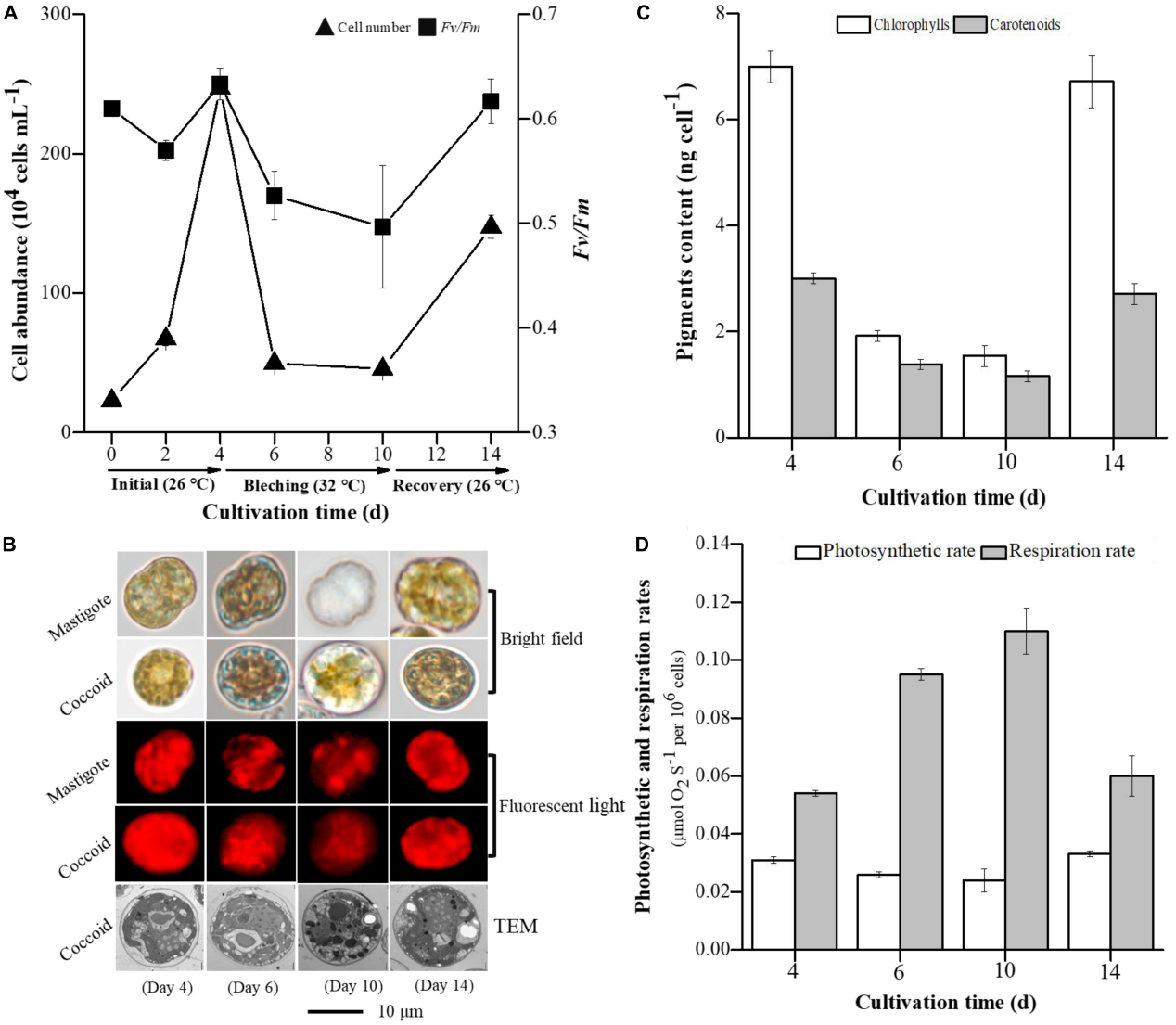

FIGURE 2 | Variations in cell abundance and *Fv/Fm* **(A)**, cell morphology **(B)**, pigment content **(C)**, photosynthesis and respiration rates **(D)** in *E. voratum* SCS01 during the photobleaching and recovery experiment. To monitor the photobleaching and recovery of *E. voratum* SCS01, the cells were initially cultured under their optimal growth temperature (26°C, initial period). The cells were exposed to thermal stress (32°C, bleached period). After incubation under thermal stress, the cells were transferred to their optimal growth temperature again (26°C, recovery period).

to the initial day 4 samples, q-value < 0.001), the meiotically up-regulated gene 158 protein (2.7-fold downregulation in day 10 bleaching samples compared to the initial day 4 samples, q-value < 0.001) and meiotic recombination protein DMC1-like subunits (2.7-fold downregulation in day 10 bleaching samples compared to the day 4 initial samples, q-value < 0.001), which may be involved in meiosis, showed decreased expression with increasing temperature (**Figure 3C**).

The abundance of genes involved in pigment metabolism, photosynthesis, respiration, carbohydrate metabolism and antioxidant activities at different temperatures was also compared (**Figure 4** and **Supplementary File 5**). During the bleaching period, genes involved in carotenoid synthesis (i.e., CHLP and VDE) were significantly downregulated (over twofold downregulation in day 10 bleaching samples compared to the initial day 4 samples, q-value < 0.001), and genes related to carotenoid degradation (i.e., carotenoid 9,10 cleavage dioxygenase 1 and the pheophytinase (PPH) responsible for chlorophyll and carotenoid cleavage) were upregulated (over twofold upregulation in day 10 bleaching samples compared to the initial day 4 samples, q-value < 0.001) (**Figure 4A**). Thermal stress universally upregulated the transcription of genes related to photosynthesis, respiration and antioxidant activities [i.e., PsbB, PsbC, PsbD, PsbO, fucoxanthin-chlorophyll as binding protein (FCPA), light harvesting chlorophyll (LHC), PsaA, PsaB, ATPF1B, and ATPF1A, involved in chloroplast photosynthesis; cyclooxygenase 1 (COX1), COX2, COX3, and ATP5O and ATP5E of ATPase, involved in mitochondrial respiration; and

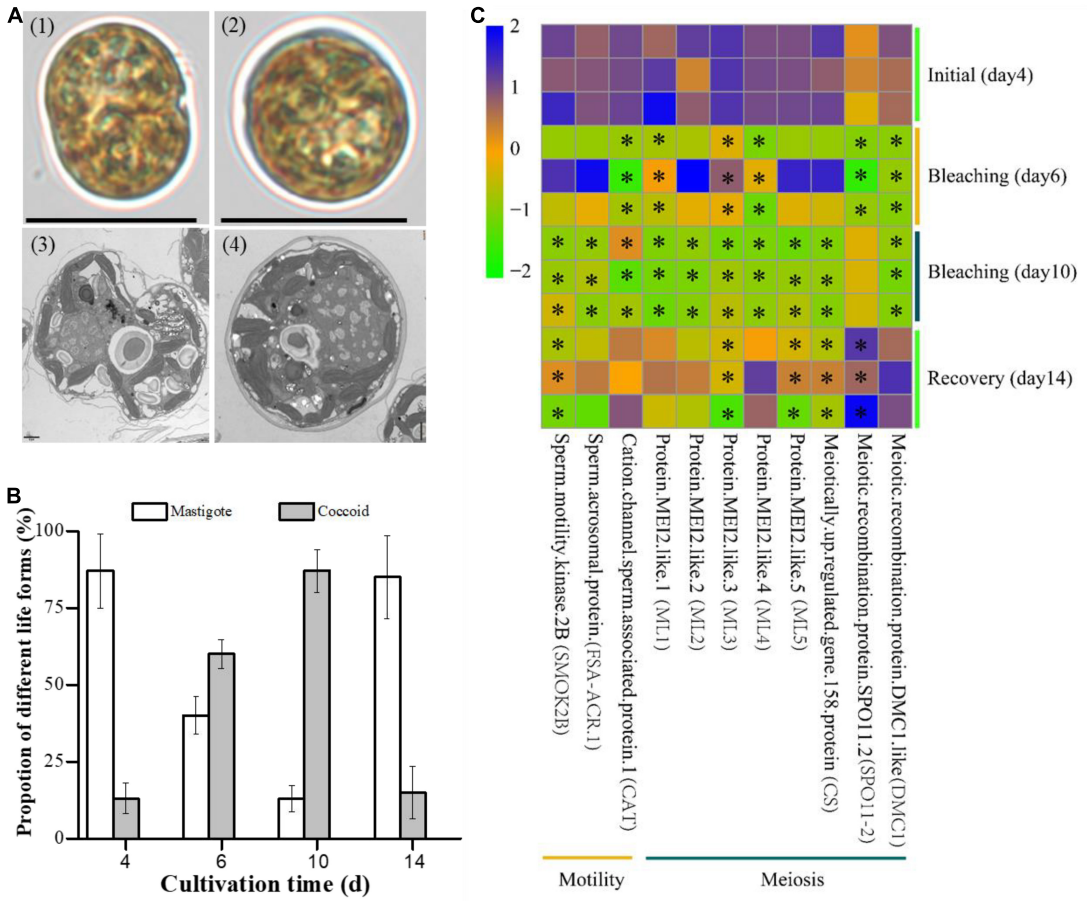

FIGURE 3 | The life forms of *E. voratum* SCS01 and genes related to these life forms during the photobleaching and recovery experiment. **(A)** Representative micrographs under bright-field conditions (top) and transmission electron micrographs (bottom) of the two major life forms observed in *E. voratum* SCS01 cells [1- and 3-mastigote cells (flagellated) and 2- and 4-coccoid cells (vegetative)]. **(B)** The proportions of mastigote cells and coccoid cells on day 4 (26°C, initial period), day 6 (32°C, bleached period), day 10 (32°C, bleached period), and day 14 (26°C, recovery period). **(C)** Pheatmap of differentially transcribed genes possibly related to life form formation. The pheatmap was drawn based on the FPKM values of differentially transcribed genes on day 4 (26°C, initial period), day 6 (32°C, bleached period), day 10 (32°C, bleached period), and day 14 (26°C, recovery period). Asterisks indicate significantly transcribed genes in the bleached period or recovery period vs. the initial period (q-value < 0.001).

HSP70, superoxide dismutase (SOD) and chloramphenicol acetyltransferase (CAT), involved in antioxidant activities] (**Figures 4A,B**). The genes encoding cytochrome b-c1 complex subunit Rieske-2 (UQCRFS1), NADH dehydrogenase beta subcomplex subunit 2 and ATP synthase subunit epsilon (mitochondrial, ATP5E) were upregulated over 7-fold in bleaching samples on day 10 compared to the initial samples on day 4 (q-value < 0.001). The genes encoding HSP70, SOD and CAT were upregulated over 5.5-fold in bleaching samples on day 10 compared to the initial samples on day 4 (q-value < 0.001).

For carbohydrate metabolism, we observed the downregulation of genes encoding proteins related to CO_2 fixation and starch and cellulose synthesis [i.e., ribulose bisphosphate carboxylase large chain precursor (RBCL), starch synthase 1 (SS1) and callose synthase (CALS)] and the upregulation of genes encoding proteins related to lipid synthesis (i.e., MCAT, HSD17B4, and ASAH2) under thermal stress (**Figure 4A**). The expression of genes during the recovery period exhibited a recovery trend when *E. voratum* SCS01 was cultured at the optimal temperature (26°C) again, except for several genes related to photosynthesis and carbohydrate metabolism (**Figure 4A**).

DISCUSSION

Photobleaching of *E. voratum* SCS01 Cells Under Thermal Stress

Increasing the temperature from 20 to 32°C altered the growth of free-living *E. voratum* SCS01, and notable photosynthesis inhibition occurred at 32°C (**Figure 1** and **Supplementary Figure 2**). This phenomenon of photosynthesis inhibition under elevated temperature was also observed in *Symbiodinium* and *Breviolum*, but not in *Durusdinium* and *Fugacium* (Takahashi et al., 2013; Karim et al., 2015). These results suggest that the sensitivity of PSII (*Fv/Fm*) to elevated temperature

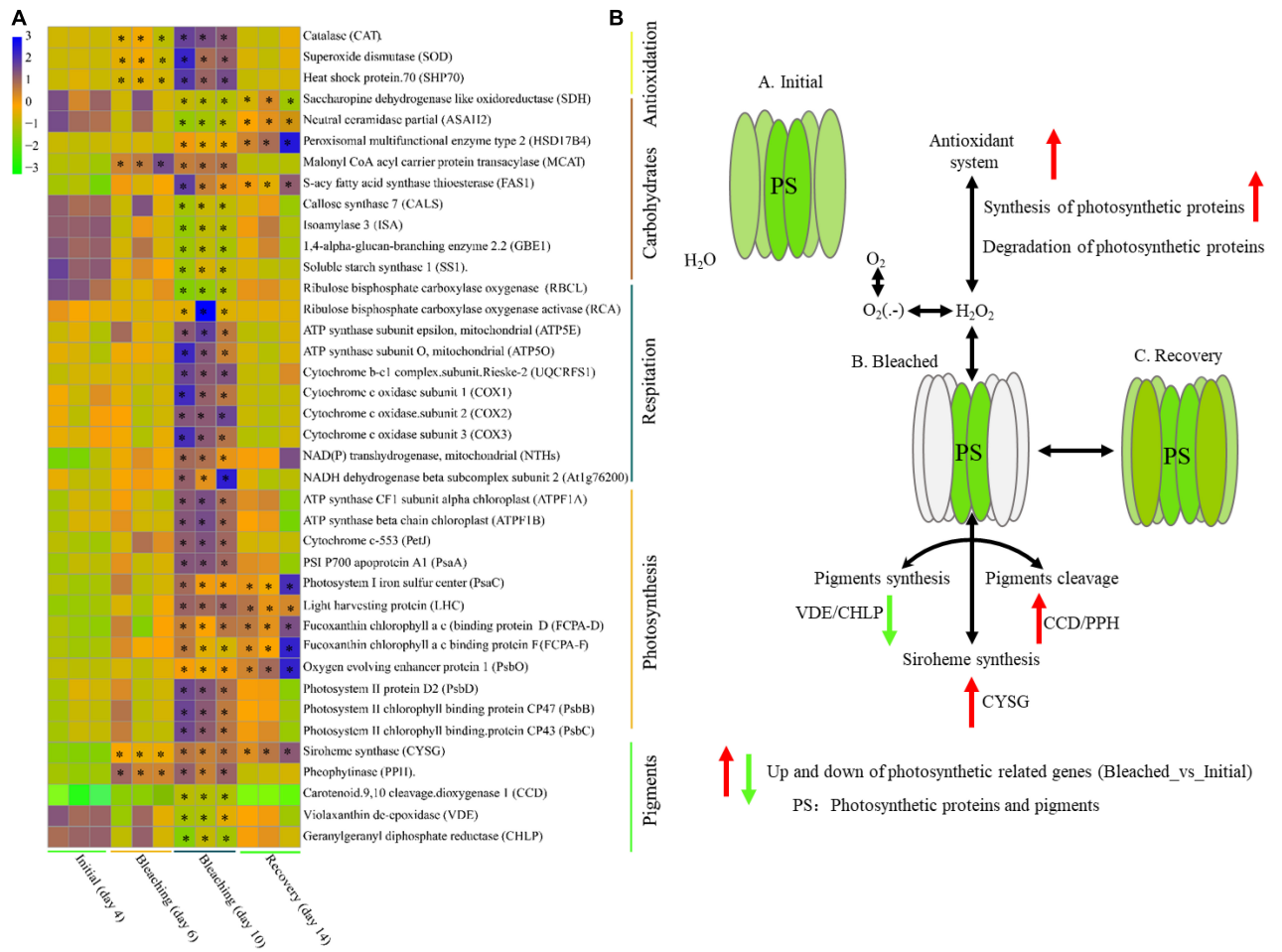

FIGURE 4 | Differential transcription of photosynthesis-related genes during the bleaching and recovery experiment. **(A)** Pheatmap of differentially transcribed genes involved in pigment metabolism, photosynthesis, respiration, carbohydrate metabolism and antioxidant activity. **(B)** Scheme illustrating the effect of thermal stress on the photobleaching and recovery of *E. voratum* SCS01 cells. The pheatmap was drawn based on the FPKM values of differentially transcribed genes on day 4 (26°C, initial period), day 6 (32°C, bleached period), day 10 (32°C, bleached period), and day 12 (26°C, recovery period). Stars indicate significantly transcribed genes in the bleached period or recovery period vs. the initial period (*q*-value < 0.001).

differs among Symbiodiniaceae phylotypes. The researchers responsible for earlier findings revealed that photoinhibition of Symbiodiniaceae is largely an impairment of PSII due to ROS production caused by high irradiance during thermal stress with the rate of photoinactivation of the core PSII proteins exceeding the rate of repair (Rehman et al., 2016; Goyen et al., 2017; Lesser, 2019). At the gene transcriptional level, we observed that antioxidant activity-related genes (i.e., genes encoding HSP70, SOD and CAT) and photosynthesis-related genes (i.e., genes encoding PsbB, PsbC, PsbD, PsbO, FCPA, and LHC in PSII; PsaA and PsaC in PSI; ATPF1B and ATPF1A of ATPase in chloroplasts) were significantly upregulated under thermal stress (**Figure 4**, especially at day 10), which is uncorrelated with declines in *Fv/Fm*. Thus, the observed photoinhibition of *E. voratum* SCS01 in this study is likely due to that the repair mechanism via antioxidant-related system does not match the rate of photoinactivation of the core PSII proteins and other photosynthetic related proteins. The previous study has been inferred that initial damage to the carbon fixation (dark reactions) at bleaching-relevant temperatures resulted in an electron sink limitation and, consequently, PSII photoinhibition (Jones et al., 1998). In this study, we observed that the gene encoding the Rubisco (RBCL) for carbon fixation was significantly downregulated, but the gene encoding Ribulose bisphosphate carboxylase/oxygenase activase (RCA) was significantly upregulated under thermal stress (**Figure 4**, especially at day 10), suggesting Rubisco activity is heat sensitive and it might be regulated by Rubisco activase in *E. voratum* SCS01. Furthermore, we initially observed significant photosynthesis inhibition of *E. voratum* SCS01 under thermal stress (at day 6), but the degree of photosynthesis inhibition was alleviated in *E. voratum* SCS01 at day 10 (**Figure 2**). Together, these results indicated that *E. voratum* SCS01 cells exhibited thermal acclimation potential as well, which involved the repair of photosynthetic related proteins via antioxidant systems.

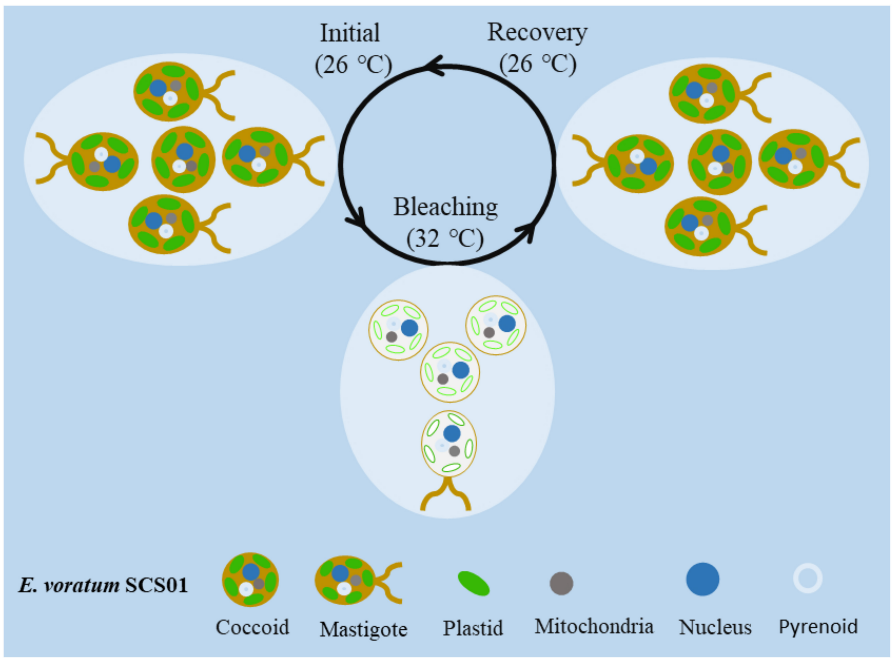

FIGURE 5 | A proposed model of photobleaching and life form transformation in seawater and host cells following short-term thermal stress-induced bleaching and recovery.

We also observed dramatic loss of photosynthetic pigments and/or plastid photobleaching under thermal stress. The pigment content of free-living Symbiodiniaceae *E. voratum* SCS01 was dramatically reduced, and the plastids of *E. voratum* SCS01 were bleached at 32°C. For symbiotic Symbiodiniaceae cells isolated from corals, previous studies showed that *Symbiodinium* sp. CCMP827 lost 50% of its initial pigment content at 34°C (Takahashi et al., 2013), but *Symbiodinium* sp. (Avir) tolerated a wide range (10–35°C) of temperatures (Pierangelini et al., 2020). These results indicated that Symbiodiniaceae taxa exhibited different photobleaching threshold temperatures, which caused a dramatic loss of photosynthetic pigments and/or plastid photobleaching. The transcriptomic analysis of *E. voratum* SCS01 under thermal stress revealed an increase in the expression of genes involved in chlorophyll and carotenoid breakdown. These results supported the conclusion from previous studies that the degradation of pigments under thermal stress is an important reason for algal photobleaching (Asada, 2004; Andreeva et al., 2007; Takahashi et al., 2013). The present study further found that genes (i.e., genes encoding CHLP and VDE) related to the biosynthesis of carotenoids were significantly downregulated under high-temperature stress. This upregulation indicated that thermal stress caused photobleaching of *E. voratum* SCS01 via the degradation of pigments and the slowing of carotenoid biosynthesis.

Recovery of *E. voratum* SCS01 Cells After Short-Term Thermal Stress

The present study observed that bleached *E. voratum* SCS01 cells recovered their photosynthesis activity and brownish color quickly after the thermal stress was removed (**Figure 2**). Notably, we observed that the proportions of different *E. voratum* life forms changed during photobleaching and recovery (**Figures 3**, **5**). The main life forms of Symbiodiniaceae include coccoid cells (vegetative) and mastigote cells (flagellated) (Fitt and Trench, 1983). The motility of mastigote cells of Symbiodiniaceae is the main characteristic of the free-living state (Fitt and Trench, 1983). Therefore, the proportions of mastigote cells accounted for approximately 85% of the total *E. voratum* SCS01 cells under the optimum growth temperature of 26°C in the present study. However, the proportion of coccoid cells significantly increased and mastigote cells significantly decreased when the temperature increased from 26°C (day 4) to 32°C (day 10). After removal of the thermal stress, the proportion of coccoid cells significantly decreased and the mastigote cells recovered to initial levels. These results suggested that coccoid cells are more tolerant to short-term thermal stress than mastigote cells of *E. voratum*. Gene transcription analysis observed that genes related to antioxidant activities (i.e., HSP70, SOD, and CAT) and respiration recovered quickly, and genes related to pigment metabolism (i.e., CCD, VDE, and CHLP), carbohydrate metabolism and photosynthesis partially recovered to their initial levels after the removal of thermal stress. The genes encoding a sperm motility kinase, sperm acrosomal protein and cation channel sperm-associated protein also exhibited recovery trends. These genes play important roles in flagellated sperm motility and development (Bissonnette et al., 2009) and may be involved in the decrease in the

proportion of mastigote cells under high-temperature stress. The functions of mastigote cells appear to include migration and grazing on bacteria and other unicellular eukaryotes (Jeong et al., 2012), which suggests that short-term high temperature affects the movement ability and feeding behavior of Symbiodiniaceae, but it recovers after the removal of thermal stress.

CONCLUSION

The present study focused on the physiological, cellular and molecular landscapes related to the photobleaching and recovery of free-living Symbiodiniaceae *E. voratum* SCS01 following short-term thermal stress. We observed that photosynthesis inhibition in *E. voratum* SCS01 cells due to thermal stress may be alleviated by prior thermal treatment, which suggests that the photosynthesis inhibition of *E. voratum* SCS01 cells could be alleviated by the short-term thermal acclimation. Our results indicate that the photobleaching of *E. voratum* SCS01 cells involves increased pigment degradation in plastids and a reduced rate of carotenoid biosynthesis. After the removal of thermal stress, the photobleached *E. voratum* SCS01 cells rapidly recovered. Most importantly, we report for the first time that thermal stress induced the transformation of the dominant life form of *E. voratum* SCS01 from mastigote cells to coccoid cells. Mastigote cells appeared to include migration and grazing on bacteria and other unicellular eukaryotes. Therefore, the decrease in mastigote cells suggests that thermal stress affects the movement ability and feeding behavior of Symbiodiniaceae. Overall, our results provide new insights into how free-living Symbiodiniaceae survive in the warming ocean via different mechanisms, most importantly by the transformation of their life form.

DATA AVAILABILITY STATEMENT

The datasets presented in this study can be found in online repositories. The names of the repository/repositories and accession number(s) can be found below: NCBI (accession: PRJNA699996).

AUTHOR CONTRIBUTIONS

SG: conceptualization, investigation, methodology, formal analysis, and writing—original draft. GL: visualization and writing—review and editing. XJ: investigation, methodology, and writing—original draft. DQ, JL KY, and XM: investigation, writing—review and editing. YT: resources, writing—review and editing. XX: resources, formal analysis, writing—review and editing, supervision, and funding acquisition. All authors contributed to the article and approved the submitted version.

FUNDING

This work was supported by the National Natural Science Foundation of China (41906135 and 31971501), the Key Special Project for Introduced Talents Team of Southern Marine Science and Engineering Guangdong Laboratory (Guangzhou) (GML2019ZD0405), and the CAS Pioneer Hundred Talents Program (Y8SL031001 and Y9YB021001).

SUPPLEMENTARY MATERIAL

The Supplementary Material for this article can be found online at: https://www.frontiersin.org/articles/10.3389/fmars.2021.740416/full#supplementary-material

REFERENCES

Andreeva, A., Abarova, S., Stoitchkova, K., Picorel, R., and Velitchkova, M. (2007). Selective photobleaching of chlorophylls and carotenoids in photosystem I particles under high-light treatment. *Photochem. Photobiol.* 83, 1301–1307. doi: 10.1111/j.1751-1097.2007.00136.x

Asada, K. (2004). "Radical production and scavenging in the chloroplasts," in *Photosynthesis and the Environment Advances in Photosynthesis and Respiration*, ed. N. R. Baker (Dordrecht: Kluwer Academic Publishers), 123–150. doi: 10.1007/0-306-48135-9_5

Bissonnette, N., Lévesque-Sergerie, J.-P., Thibault, C., and Boissonneault, G. (2009). Spermatozoal transcriptome profiling for bull sperm motility: a potential tool to evaluate semen quality. *Reproduction* 138, 65–80. doi: 10.1530/REP-08-0503

Buerger, P., Alvarez-Roa, C., Coppin, C. W., Pearce, S. L., Chakravarti, L. J., Oakeshott, J. G., et al. (2020). Heat-evolved microalgal symbionts increase coral bleaching tolerance. *Sci. Adv.* 6:eaba2498. doi: 10.1126/sciadv.aba2498

Chang, F. H. (1983). Winter phytoplankton and microzooplankton populations off the coast of Westland, New Zealand, 1979. *N. Z. J. Mar. Freshw. Res.* 17, 279–304. doi: 10.1080/00288330.1983.9516003

Dere,Ş, Güneş, T., and Sivaci, R. (1998). Spectrophotometric determination of chlorophyll–A, B and total carotenoid contents of some algae species using different solvents. *Botany* 22, 13–17.

DuBois, M., Gilles, K. A., Hamilton, J. K., Rebers, P. A., and Smith, F. (1956). Colorimetric method for determination of sugars and related substances. *Anal. Chem.* 28, 350–356. doi: 10.1021/ac60111a017

Fitt, W. K., and Trench, R. K. (1983). "Infection of coelenterate hosts with the symbiotic dinoflagellate *Symbiodinium microadriaticum*," in *Intracellular Space as Oligogenetic Ecosystem*, eds H. E. A. Schenk and W. Schwemmler (Berlin: De Gruyter), 675–682. doi: 10.1515/9783110841237-070

Freudenthal, H. D. (1962). *Symbiodinium* gen. nov. and *Symbiodinium microadriaticum* sp. nov., a zooxanthella: taxonomy, life cycle, and morphology. *J. Protozool.* 9, 45–52. doi: 10.1111/j.1550-7408.1962.tb02579.x

Gong, S., Chai, G., Sun, W., Zhang, F., Yu, K., and Li, Z. (2021). Global-scale diversity and distribution characteristics of reef-associated symbiodiniaceae via the cluster-based parsimony of internal transcribed spacer 2 sequences. *J. Ocean Univ. China* 20, 296–306. doi: 10.1007/s11802-021-4364-5

Gong, S., Chai, G., Xiao, Y., Xu, L., Yu, K., Li, J., et al. (2018). Flexible symbiotic associations of *Symbiodinium* with five typical coral species in tropical and subtropical reef regions of the northern South China Sea. *Front. Microbiol.* 9:2485. doi: 10.3389/fmicb.2018.02485

Gong, S., Jin, X., Xiao, Y., and Li, Z. (2020). Ocean acidification and warming lead to increased growth and altered chloroplast morphology in the thermo-tolerant alga *Symbiochlorum hainanensis*. *Front. Plant Sci.* 11:585202. doi: 10.3389/fpls.2020.585202

Gong, S., Xu, L., Yu, K., Zhang, F., and Li, Z. (2019). Differences in symbiodiniaceae communities and photosynthesis following thermal bleaching of massive corals

in the northern part of the South China Sea. *Mar. Pollut. Bull.* 144, 196–204. doi: 10.1016/j.marpolbul.2019.04.069

Goyen, S., Pernice, M., Szabó, M., Warner, M. E., Ralph, P. J., and Suggett, D. J. (2017). A molecular physiology basis for functional diversity of hydrogen peroxide production amongst *Symbiodinium* spp. (Dinophyceae). *Mar. Biol.* 164:46. doi: 10.1007/s00227-017-3073-5

Guillard, R. R. L., and Ryther, J. H. (1962). Studies of marine planktonic diatoms: i. *Cyclotella nana* hustedt, and detonula confervacea (cleve) gran. *Can. J. Microbiol.* 8, 229–239. doi: 10.1139/m62-029

Haas, B. J., Papanicolaou, A., Yassour, M., Grabherr, M., Blood, P. D., Bowden, J., et al. (2013). De novo transcript sequence reconstruction from RNA-seq using the Trinity platform for reference generation and analysis. *Nat. Protoc.* 8, 1494–1512. doi: 10.1038/nprot.2013.084

Hill, R., Szabó, M., Rehman, A., Vass, I., Ralph, P. J., and Larkum, A. W. D. (2014). Inhibition of photosynthetic CO2 fixation in the coral *Pocillopora damicornis* and its relationship to thermal bleaching. *J. Exp. Biol.* 217(Pt 12), 2150–2162. doi: 10.1242/jeb.100578

Jeans, J., Szabo, M., Campbell, D. A., Larkum, A. W. D., Ralph, P. J., and Hill, R. (2014). Thermal bleaching induced changes in photosystem II function not re?ected by changes in photosystem II protein content of *Stylophora pistillata*. *Coral Reefs* 33, 131–139. doi: 10.1007/s00338-013-1091-4

Jeong, H. J., Lee, S. Y., Kang, N. S., Yoo, Y. D., Lim, A. S., Lee, M. J., et al. (2014). Genetics and morphology characterize the dinoflagellate *Symbiodinium voratum* , n. sp., (Dinophyceae) as the sole representative of *Symbiodinium Clade* E. *J. Eukaryot. Microbiol.* 61, 75–94. doi: 10.1111/jeu.12088

Jeong, H. J., Yoo, Y. D., Kang, N. S., Lim, A. S., Seong, K. A., Lee, S. Y., et al. (2012). Heterotrophic feeding as a newly identified survival strategy of the dinoflagellate *Symbiodinium*. *Proc. Natl. Acad. Sci. U.S.A.* 109, 12604–12609. doi: 10.1073/pnas.1204302109

Jones, R. J., Hoegh-Guldberg, O., Larkum, A. W. D., and Schreiber, U. (1998). Temperature-induced bleaching of corals begins with impairment of the CO2 fixation mechanism in zooxanthellae. *Plant Cell Environ.* 21, 1219–1230. doi: 10.1046/j.1365-3040.1998.00345.x

Karim, W., Nakaema, S., and Hidaka, M. (2015). Temperature effects on the growth rates and photosynthetic activities of *Symbiodinium* cells. *J. Mar. Sci. Eng.* 3, 368–381. doi: 10.3390/jmse3020368

Khozingoldberg, I., Shrestha, P., and Cohen, Z. (2005). Mobilization of arachidonyl moieties from triacylglycerols into chloroplastic lipids following recovery from nitrogen starvation of the microalga *Parietochloris incisa*. *Biochim. Biophys. Acta* 1738, 63–71. doi: 10.1016/j.bbalip.2005.09.005

LaJeunesse, T. C., Parkinson, J. E., Gabrielson, P. W., Jeong, H. J., Reimer, J. D., Voolstra, C. R., et al. (2018). Systematic revision of symbiodiniaceae highlights the antiquity and diversity of coral endosymbionts. *Curr. Biol.* 28, 2570–2580.e6. doi: 10.1016/j.cub.2018.07.008

Lesser, M. P. (2019). Phylogenetic signature of light and thermal stress for the endosymbiotic dinoflagellates of corals (family Symbiodiniaceae). *Limnol. Oceanogr.* 64, 1852–1863. doi: 10.1002/lno.11155

Li, B., and Dewey, C. N. (2011). RSEM: accurate transcript quantification from RNA-Seq data with or without a reference genome. *BMC Bioinformatics* 12:323. doi: 10.1186/1471-2105-12-323

Li, T., Yu, L., Chen, X., Lin, X., Li, L., Guo, C., et al. (2021). Remarkable metabolic reconfiguration due to N deficiency and an ammonium-to-nitrate shift in the free-living *Effrenium voratum* (Symbiodiniaceae). J. *Geophys. Res. Biogeosciences* 126, 1–15. doi: 10.1029/2020JG006172

Mou, S., Zhang, Y., Li, G., Li, H., Liang, Y., Tang, L., et al. (2017). Effects of elevated CO2 and nitrogen supply on the growth and photosynthetic physiology of a marine cyanobacterium, *Synechococcus* sp. PCC7002. *J. Appl. Phycol.* 29, 1755–1763. doi: 10.1007/s10811-017-1089-3

Pierangelini, M., Thiry, M., and Cardol, P. (2020). Different levels of energetic coupling between photosynthesis and respiration do not determine the occurrence of adaptive responses of symbiodiniaceae to global warming. *New Phytol.* 228, 855–868. doi: 10.1111/nph.16738

Pochon, X., Putnam, H. M., and Gates, R. D. (2014). Multi-gene analysis of *Symbiodinium* dinoflagellates: a perspective on rarity, symbiosis, and evolution. *PeerJ* 2:e394. doi: 10.7717/peerj.394

Rehman, A. U., Szabó, M., Deák, Z., Sass, L., Larkum, A., Ralph, P., et al. (2016). *Symbiodinium* sp. cells produce light-induced intra- and extracellular singlet oxygen, which mediates photodamage of the photosynthetic apparatus and has the potential to interact with the animal host in coral symbiosis. *New Phytol.* 212, 472–484. doi: 10.1111/nph.14056

Rosic, N. N., and Hoegh-Guldberg, O. (2010). A method for extracting a high-quality RNA from *Symbiodinium* sp. *J. Appl. Phycol.* 22, 139–146. doi: 10.1007/s10811-009-9433-x

Rowan, R., and Powers, D. (1991). Molecular genetic identification of symbiotic dinoflagellates (zooxanthellae). *Mar. Ecol. Prog. Ser.* 71, 65–73. doi: 10.3354/meps071065

Sully, S., Burkepile, D. E., Donovan, M. K., Hodgson, G., and van Woesik, R. (2019). A global analysis of coral bleaching over the past two decades. *Nat. Commun.* 10:1264. doi: 10.1038/s41467-019-09238-2

Szabó, M., Larkum, A. W. D., Suggett, D. J., Vass, I., Sass, L., Osmond, B., et al. (2017). Non-intrusive assessment of photosystem II and photosystem I in whole coral tissues. *Front. Mar. Sci.* 4:269. doi: 10.3389/fmars.2017.00269

Takahashi, S., Yoshioka-Nishimura, M., Nanba, D., and Badger, M. R. (2013). Thermal acclimation of the symbiotic alga *Symbiodinium* spp. alleviates photobleaching under heat stress. *Plant Physiol.* 161, 477–485. doi: 10.1104/pp.112.207480

Tian-Tian, L., Ping, H., Jia-Xing, L., Zhi-Xin, K., and Ye-Hui, T. (2019). Utilization of different dissolved organic phosphorus sources by *Symbiodinium voratum* in vitro. *FEMS Microbiol. Ecol.* 95:fiz150. doi: 10.1093/femsec/fiz150

van Kooten, O., and Snel, J. F. H. (1990). The use of chlorophyll fluorescence nomenclature in plant stress physiology. *Photosynth. Res.* 25, 147–150. doi: 10.1007/BF00033156

Xiang, T., Hambleton, E. A., DeNofrio, J. C., Pringle, J. R., and Grossman, A. R. (2013). Isolation of clonal axenic strains of the symbiotic dinoflagellate *Symbiodinium* and their growth and host specificity 1. *J. Phycol.* 49, 447–458. doi: 10.1111/jpy.12055

Yamashita, H., and Koike, K. (2013). Genetic identity of free-living *Symbiodinium* obtained over a broad latitudinal range in the Japanese coast: phylogeny of free-living *Symbiodinium*. *Phycol. Res.* 61, 68–80. doi: 10.1111/pre.12004

Conflict of Interest: The authors declare that the research was conducted in the absence of any commercial or financial relationships that could be construed as a potential conflict of interest.

Publisher's Note: All claims expressed in this article are solely those of the authors and do not necessarily represent those of their affiliated organizations, or those of the publisher, the editors and the reviewers. Any product that may be evaluated in this article, or claim that may be made by its manufacturer, is not guaranteed or endorsed by the publisher.